Structure, Vol. 9, 1017–1027, November, 2001, ©2001 Elsevier Science Ltd. All rights reserved. PII S0969-2126(01)00667-0

# Single-Site Mutations Induce 3D Domain Swapping in the B1 Domain of Protein L from *Peptostreptococcus magnus*

**Jason W. O'Neill,[1,2] David E. Kim,[3] Keyji Johnsen,[1] David Baker,[3] and Kam Y.J. Zhang[1,4,5]**
[1] Division of Basic Sciences
Fred Hutchinson Cancer Research Center
1100 Fairview Avenue North
Seattle, Washington 98109
[2] Molecular and Cellular Biology Program and
[3] Department of Biochemistry
University of Washington
Seattle, Washington 98195

## Summary

**Background:** Thermodynamic and kinetic studies of the Protein L B1 domain (PpI) suggest a folding pathway in which, during the folding transition, the first β hairpin is formed while the second β hairpin and the α helix are largely unstructured. The same mutations in the two β turns have opposite effects on the folding and unfolding rates. Three of the four residues composing the second β turn in PpI have consecutive positive $\phi$ angles, indicating strain in the second β turn.

**Results:** We have determined the crystal structures of the β turn mutants G55A, K54G, and G15A, as well as a core mutant, V49A, in order to investigate how backbone strain affects the overall structure of PpI. Perturbation of the hydrophobic interactions at the closed interface by the V49A mutation triggered the domain swapping of the C-terminal β strand that relieved the strain in the second β turn. Interestingly, the asymmetric unit of V49A contains two monomers and one domain-swapped dimer. The G55A mutation escalated the strain in the second β turn, and this increased strain shifted the equilibrium toward the domain-swapped dimer. The K54G structure revealed that the increased stability is due to the reduction of strain in the second β turn, while the G15A structure showed that increased strain alone is insufficient to trigger domain swapping.

**Conclusions:** Domain swapping in PpI is determined by the balance of two opposing components of the free energy. One is the strain in the second β turn that favors the dimer, and the other is the entropic cost of dimer formation that favors the monomer. A single-site mutation can disrupt this balance and trigger domain swapping.

## Introduction

Many proteins have the ability to self assemble into dimers or oligomers through an exchange of structural elements. One form of exchange, which is quite often reversible, is 3D domain-swapping (DS). This event requires the breaking of noncovalent interactions of one monomer's domain or secondary-structural elements, which are replaced by an identical domain from another molecule to form a dimer or oligomer [1, 2]. Domain swapping has been proposed as a possible mechanism for protein aggregation and amyloid formation [3, 4], as well as regulation of function or activity [5–7].

A growing number of domain-swapped proteins have been discovered. These include RNase A [8, 9] and BS-RNase [10], Cro [11], Spectrin [12], and the bovine odorant binding protein [13], as well as the mammalian cell cycle regulatory subunit protein CksHs1 [14] and its yeast homolog p13suc1 [15]. Domain swapping was first observed on a molecular level by Eisenberg and coworkers in 1994 [16], when they found that acidic conditions disrupted ionic interactions between two domains in diphtheria toxin and stabilized a domain-swapped conformation. Low pH is a common trigger for domain swapping as well as amyloid formation. Other mechanisms that are thought to help the transition from monomer to domain-swapped dimer include mild denaturation, elevation of protein concentration, and conformational strain.

The introduction of mutations, additions, or deletions in the hinge-loop can induce conformational strain and induce domain swapping. The hinge-loop region is a short polypeptide segment that links the swapped domains of the dimer and is usually a loop in the monomer. When domain-swapped, the hinge is in a different conformation than it is in the monomer. The role of a hinge-loop in controlling protein quaternary structure is highlighted in domain swapping. For example, a deletion of six residues in a surface loop of staphylococcal nuclease transforms the monomeric protein into a domain-swapped dimer, in which the carboxy-terminal α helix is exchanged [17]. The dimeric βB2-Crystallin differs from the monomeric γB-Crystallin in having an acidic residue in the hinge-loop and an Asp residue located in the main body of the protein. This electrostatic repulsion prevents βB2-Crystallin from forming a closed monomer and causes it to domain swap [18]. Naturally occurring backbone conformational strain induced by two conserved prolines in the hinge-loop region of p13suc1 has been shown to be the mechanism by which this protein switches between monomeric and domain-swapped states [19, 20].

In this paper we explore the role of conformational strain imposed by β turn residues in the regulation of domain swapping. We use the 64 residue B1 domain of Protein L (PpI) from *Peptostreptococcus magnus,* which consists of a central α helix packed against a four-stranded β sheet formed by two β hairpins [21, 22]. The topology of PpI appears to be pseudo-symmetrical. However, the same substitution (G15A and G55A) in the pseudo-symmetrically disposed first and second β turns had opposite effects on the folding/unfolding kinetics of PpI [23]. Although both substitutions had similar de-

[4] Correspondence: kzhang@stromix.com
[5] Present address: Structural GenomiX, 10505 Roselle Street, San Diego, California 92121.

**Key words:** Protein L B1 domain; strained β hairpin turn; positive phi angles; domain swapping; amyloid formation

Table 1. Structure Determination Statistics

| Diffraction Data Statistics | | | | |
|---|---|---|---|---|
| Data set | V49A | G55A | K54G | G15A |
| Unit cell (Å): A = | 53.13 | 48.01 | 66.63 | 66.50 |
| B = | 53.13 | 15.12 | 66.63 | 66.50 |
| C = | 115.51 | 60.09 | 108.83 | 109.19 |
| Space group | $P4_1$ | $C222_1$ | $P3_221$ | $P3_221$ |
| Resolution (Å) | 1.8 | 1.8 | 1.8 | 2.1 |
| Observations | 134,022 | 58,197 | 1,330,332 | 109,046 |
| Unique reflections | 29,286 | 10,272 | 26,473 | 16,901 |
| Completeness (%) | 98.7 | 98.6 | 99.7 | 99.9 |
| I/sigma | 30.9 | 31.6 | 16 | 9.6 |
| $R_{merge}$ (%)[1] | 4.7 | 5.6 | 6.5 | 10.9 |
| **Refinement Statistics** | | | | |
| Resolution | 25–1.8 | 25–1.8 | 25–1.8 | 25–2.1 |
| Number of Reflections (F > 0) | 28,396 | 10,255 | 26,441 | 16,869 |
| $R_{cryst}$ ($R_{free}$)[2,3] | 21.1 (23.9) | 18.6 (21.0) | 19.9 (20.5) | 21.3 (23.0) |
| Test size (%)[3] | 9.50 | 4.80 | 5.10 | 5.00 |
| Number of molecules in asymetrical unit | 4 | 1 | 2 | 2 |
| Number of non-hydrogen atoms: | | | | |
| Protein | 1,940 | 557 | 1,122 | 1,138 |
| Zinc | 0 | 3 | 8 | 8 |
| Water | 122 | 168 | 213 | 171 |
| B factor (Å$^2$) | 31 | 26.9 | 23.3 | 21.5 |
| Rmsd from ideal values: | | | | |
| Bond length (Å) | 0.0057 | 0.0041 | 0.0052 | 0.0056 |
| Bond angles (°) | 1.25 | 1.26 | 1.25 | 1.28 |
| Ramachandran plot[4] | | | | |
| Residues in most-favored & (disallowed) regions (%)[5] | 96 (0) | 98.6 (0) | 96 (0) | 95 (0) |

[1] $R_{merge} = \sum_{hkl}\sum_{i} (|I^i_{hkl} - \langle I_{hkl}\rangle|)/\sum_{hkl} \langle I_{hkl}\rangle$, where $I^i_{hkl}$ is the intensity of an individual measurement of the reflection with Miller indices $h$, $k$, and $l$, and $\langle I_{hkl}\rangle$ is the mean intensity of that reflection.

[2] $R_{cryst} = \sum_{hkl} (|F^o_{hkl} - F^c_{hkl}|/F^o_{hkl})$ where $F^o_{hkl}$ and $F^c_{hkl}$ are the observed and calculated structure factor amplitudes.

[3] $R_{free}$ [43] is equivalent to $R_{cryst}$ but is calculated with reflections omitted from the refinement process. The $R_{free}$ reflections were extracted with the CCP4 program FreeRflag.

[4] Calculated with the program CNS [41].

[5] Calculated with the program PROCHECK [42].

stabilizing effects on Ppl, the G55A substitution in the second β turn increased the unfolding rate by 15-fold and had only a minor effect on the folding rate, whereas the G15A substitution decreased the folding rate by 9-fold and had only minor effects on the unfolding rate. A systematic thermodynamic and kinetic study of single-site mutations spanning the entire Ppl revealed the folding transition state in which β strands 1 and 2 and the first β hairpin turn are largely structured, while β strands 3 and 4, the second β hairpin turn, and the α helix are largely disrupted [24]. The pseudo-wild-type Ppl structure (WT*) revealed that while the first β turn is a classic type I turn with only G15 having a positive $\phi$, the second β turn has a distorted type I′ conformation in which three of the four residues (D53, K54, and G55) comprising the turn have positive $\phi$ angles [22]. Positive $\phi$ angles can induce strain when the $C_\beta$ atom of a residue makes close contacts with its backbone oxygen. The above results suggest that the second β turn in WT* is in a strained conformation.

We have structurally characterized four separate residue substitutions, V49A, G55A, K54G, and G15A. We found from these structures that two opposing components of free energy exist in Ppl between the entropic cost of dimer formation and the strain in the second β turn. When Ppl was mutated to either V49A or G55A, domain swapping was observed due to dominance of the strain in the second β turn. The K54G and G15A mutations showed that the close contact between the $C_\beta$ atom of residues with positive $\phi$ angle and the backbone oxygen is a key element that induces strain in β turns.

## Results

### V49A: Equilibrium between the Monomer and the Dimer

In order to probe the local and global structural changes of Ppl upon mutations of core residues, we determined the structure of Ppl with a V49A substitution to a resolution of 1.8 Å (Table 1). The V49A mutation is located in the hydrophobic core of the protein on the third β strand and destabilizes Ppl by 0.92 kcal/mol [24]. The dominant and striking feature of the V49A asymmetric unit is that it contains two monomers and a β strand-swapped dimer (Figure 1a). While the V49A molecules A and C maintain the wild-type fold, molecules B and D form a dimer through the exchange of their fourth β strands. The electron density corresponding to the hinge region of the domain-swapped dimer is unambiguous, as can be seen from the simulated annealing composite omit maps (Figures 2a, 2b). The extended fourth β strand integrates into the dimer partner and creates a buried surface area of approximately 930 Å$^2$. Remarkably, the hydrogen

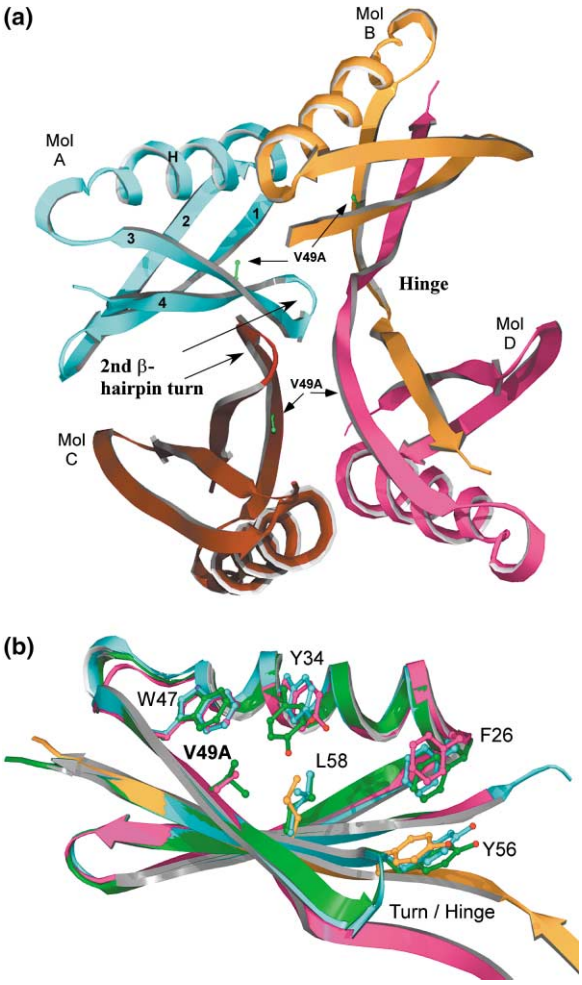


Figure 1. The Asymmetric Unit of V49A

(a) The asymmetric unit contains two monomers (cyan/brown) and a domain-swapped dimer (orange and magenta). The molecules are labeled Mol A, B, C, and D, respectively. The β strands and α helix are labeled on molecule A. Arrows point to the A49 in each molecule. The hinge region consists of the residues in the second β turn (residues 53–56).

(b) The repacking of side chains near the V49A residues for the monomer (cyan), dimer (orange/magenta), and WT (green). For the V49A monomer the side-chain of Y34 has the largest shift, similar to the V49A domain-swapped dimer. In the V49A domain-swapped dimer the side chain of Y56 shifts due to the β strand extension and causes further shifts in F26 and a 180° rotation about $\chi 1$ for L58.

bonding and atomic positions of the domain-swapped dimer are comparable to WT*.

The deletion of two methyl groups in the V49A mutation triggered a compensatory side-chain movement of several residues. In the V49A monomer, Y34, adjacent to A49, rotated to fill in for the loss of two methyl groups (Figure 1b). However, in the domain-swapped dimer the extension of the fourth β strand caused several perturbations. The movement of Y56 caused a compensatory shift in F26, and L58 rotated 180° about $\chi_1$ to make more satisfying contacts with A49, while Y34 rotated as in the monomer (Figure 2b).

Domain swapping in V49A caused minimal perturbations on the overall structure except in the hinge region of the second β turn. Comparisons against the monomeric WT* structure [22] showed that the V49A monomer has a root mean square difference (rmsd) of 0.65 Å (residues 4–63), while the V49A domain-swapped dimer has a rmsd of 0.71 Å (residues 4–50, 56′–63′). The rmsd between the V49A monomer and dimer is 0.51 Å.

In the WT* structures, the second β turn residues, D53, K54, and G55, have positive $\phi$ angles (Table 2). These angles place this turn into the left-handed α-helical region of Ramachandran space, which is statistically less populated and thus energetically less favorable than other regions [25]. Furthermore, non-glycine residues with positive $\phi$ angles tend to be destabilizing [26–28]. In the V49A structures, residues D53, K54, and G55 in the monomer formed the second β hairpin turn and retained the strain as in the WT* Ppl; however, these residues formed an extended hinge region in the domain-swapped dimer and released the strain (Figure 1a). Interestingly, the hinge region (residues 52–55) of the dimeric B molecule began its rotation (away from WT* conformation) at A52 and completed its rotation at G55, while the hinge of the D molecule began its rotation at K54 and ended it at G55 (Table 2). This backbone rotation asymmetry left D53 of the B molecule with a negative $\phi$ angle while the D53 of molecule D retained the positive $\phi$ angle in the same conformation as found in WT*, although the $\psi$ angle had moved 12°. This caused the $C_\beta$ atom of D53 in molecule D to make a close contact with its backbone oxygen (2.7 Å), creating WT*-like strain in that region. This asymmetry of $\phi$ angles in the domain-swapped dimers and the residual strain could have been due to either the internal structural restraint or the crystallographic packing.

## Domain Swapping in G55A

The domain swapping in the V49A structure suggests that there are two opposing components of free energy exerted on the second β turn and the interplay of these two opposing free energy components dictates the outcome of the conformational change. The free energy component that favors domain swapping is the strain in the second β turn as indicated by the three consecutive positive $\phi$ angles. The free energy component that disfavors domain swapping is the loss in entropy upon dimer formation. Based on the above model, we predicted that if the strain in the second β turn is increased, a domain swapped dimer should be observed. The G55A mutation significantly increased the strain in the second β turn and destabilized Ppl by 2.1 kcal/mol [24] and therefore was selected to test the above hypothesis.

The crystal structure of G55A, determined to 1.8 Å resolution (Table 1), shows the fourth β strand domain-swapping in a similar manner as in V49A dimer structure (Figure 2c and 4a). In this case the G55A structure shows only β strand-swapped dimers with the hinge residues (53–56) having all negative $\phi$ angles, unlike molecule D of V49A (Table 2). This is consistent with the greater ease with which the G55A molecules can form dimers, as seen by size exclusion chromatography (SEC; Figure 3). The $C_\beta$ of A55 and its symmetry mate in the dimer are 3.9 Å apart and tilted toward each other to make stabilizing van der Waals contacts. Furthermore, the $C_\beta$

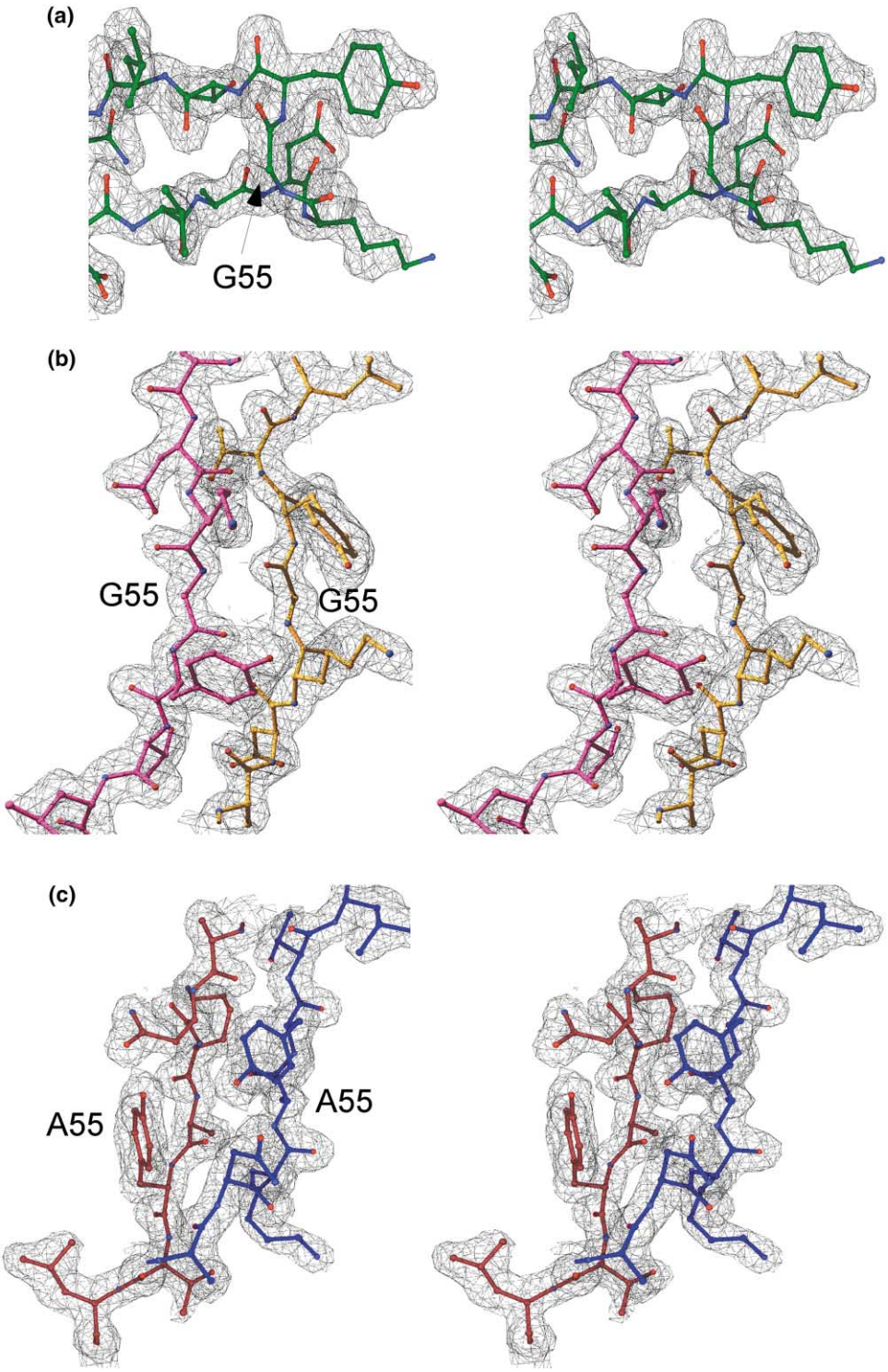


Figure 2. Stereo Views of Electron Density from Composite Omit Maps of V49A and G55A at the Second β Turn/Hinge Region

The residues near K54, G55, and Y56 are shown.

(a) Second β turn in the V49A monomer.

(b) V49A hinge region in the domain-swapped dimer.

(c) G55A domain-swapped dimer hinge region. The residue from the strand in the domain-swapped pair is denoted as G55′, for example. Non-carbon atoms are color coded with blue for nitrogen and red for oxygen. The electron density around the residue of the hinge region is contoured at 1σ.

Table 2. Dihedral Angles for Residues 53, 54, and 55

| | V49A-A | | V49A-B | | V49A-C | | V49A-D | | G55A[1] | | WT*-A[2] | |
|---|---|---|---|---|---|---|---|---|---|---|---|---|
| | $\phi$ | $\psi$ | $\phi$ | $\psi$ | $\phi$ | $\psi$ | $\phi$ | $\psi$ | $\phi$ | $\psi$ | $\phi$ | $\psi$ |
| ASP 53 | 49.73 | 48.56 | −150.7 | 150.25 | 48.08 | 47.14 | 47.79 | 61.29 | −73.26 | 152.38 | 49.01 | 48.12 |
| LYS 54 | 56.51 | 30.86 | −120.3 | 134.64 | 54.96 | 30.28 | −64.51 | 136.5 | −131.1 | −30.08 | 58.74 | 28.17 |
| GLY 55 | 96.27 | −2.03 | −131.6 | 155.98 | 103.76 | −5.38 | −158.2 | 168.91 | −153.2 | 148.73 | 98.95 | −7.08 |

[1] G55 is A55.
[2] G15A and K54G had dihedral angles in line with the A molecule of WT*.

of A55 does not clash with its backbone carbonyl oxygen. The buried surface area for residues 56–64 is 930 Å$^2$ per monomer, similar to that in the V49A domain-swapped dimer. Finally, the overlay of a monomeric unit of the G55A dimer (residues 4–50 and 56′–63′) with WT* shows an rmsd of 0.47 Å for backbone atoms. This demonstrates that the domain-swapped dimer maintains the essential monomeric contacts.

### Concentration Dependence and Slow Kinetics of G55A Domain Swapping

The G55A protein displays a two-state folding kinetics similar to the monomeric WT* and thus is modeled as a monomer in the kinetic analysis [24]. The domain-swapped dimer revealed by the crystal structure of G55A prompted us to investigate the validity of the monomeric G55A model used in the folding kinetics studies. The G55A protein at 15 μM concentration, as used for the folding kinetics studies, was denatured and then refolded immediately before injection onto SEC. The freshly refolded G55A was found to be monomeric (Figure 3d). Refolded G55A protein at 15 μM was then stored at 4°C and reanalyzed after 8 days. The G55A protein loaded at 15 μM was found to contain about 20% dimer (Figure 3c). These SEC studies of the G55A protein demonstrated that the monomeric model of G55A is valid for the kinetic studies of folding at low concentrations. It also revealed that a slow equilibrium exists between the monomeric and dimeric forms, with conversion to the dimeric form occurring even at low protein concentrations. The equilibrium is shifted in favor of the dimer with the increase of protein concentration (Figure 3a–c). There is a trace amount of dimer found in the V49A protein at 3100 μM concentration (Figure 3e). In contrast, WT remains monomeric even at high protein concentrations (Figure 3f).

Acidic pH has been reported to induce domain swapping in systems such as Diphtheria toxin and RNase A. The acidic conditions could potentially affect the domain-swapping state of PpI since the V49A protein was crystallized at pH 4.6. To analyze this we compared the dimer fraction of 600 μM G55A and 1250 μM V49A at pH 4.6 to the dimer fractions found under these concentrations at pH 7.0. We found similar dimerization states between the acidic and neutral pH for both V49A and G55A (data not shown), and these findings further indicate that conformational strain and protein concentration, rather than pH, play a major role in triggering domain swapping in both cases.

### The Hinge Regions of V49A and G55A Are not Identical

The hinge angle between the two lobes of the G55A dimer is nearly 180°. This represents approximately a 58° hinge angle difference between the G55A and V49A dimers (Figure 4b). This also demonstrates the conformational flexibility of the hinge region. Comparisons of hydrogen bonding (H bonding) patterns show further differences. Figure 5 shows comparisons of residues 52–57 from WT*, V49A, and G55A domain-swapped structures. The asymmetry of the hinge bend in V49A is reflected in its H bonding pattern. In the B molecule the H bonding pattern includes $N_{52}$ and $O_{53}$, while in the D molecule, where D53 has a positive $\phi$ angle, the H bonds include $N_{52}$ and $O_{52}$ before skipping to G55. Also in V49A, the G55 residue makes two H bonds to G55′ in the noncrystallographic symmetry-related molecule, whereas in G55A the two molecules in the dimer are related by crystallographic symmetry and the H bonding pattern is $O_{54}$-$N_{55}$ and $N_{54}$-$O_{55}$, allowing A55 to be directly across from A55′.

### K54G Reduces Strain in the Second β Hairpin Turn

We hypothesize that strain exists in the second β turn because of its positive $\phi$ angles inducing close contacts between the $C_\beta$ of D53 and K54 and their backbone carbonyl oxygens (distances as seen in WT* structures: $C_\beta$(D53)-O(D53) = 2.73 ± 0.01 Å and $C_\beta$(K54)-O(K54) = 2.77 ± 0.02 Å, [22]). Generally, nonbonded $C_\beta$ atoms are at least 2.8 Å from backbone carbonyl oxygens, and 90% of the time the distance is 3.4 Å or greater [29]. We found that strain in the second β turn is partially abrogated by a K54G substitution but not by a K54A substitution [24]. Thermodynamic and kinetic measurements showed that the K54G mutant was 0.67 kcal/mol more stable than WT*, and the K54G mutation increased the folding rate by 1.9-fold and decreased the unfolding rate by 0.6-fold. We crystallized the K54G mutant to see if relieving the strain caused by the $C_\beta$-to-carbonyl-oxygen ($C_\beta$-O) clash in K54 would have any effect on the conformation of the second β turn. The 1.8 Å structure (Table 1 and Figure 6) revealed little main-chain movement in the second β turn and confirmed that the increased stability is primarily due to the loss of the $C_\beta$ of K54 and the consequent elimination of steric clashes. The overall rmsd between K54G and WT* (A molecules) is 0.43 Å, and the rmsd between the four residues of the second β turn is 0.41 Å. The $\phi$ angles for D53, G54, and G55 remained positive, and the $C_\beta$-O distance for D53 remained at 2.72 Å. This suggests that the stability gained is primarily due to the removal of the close con-

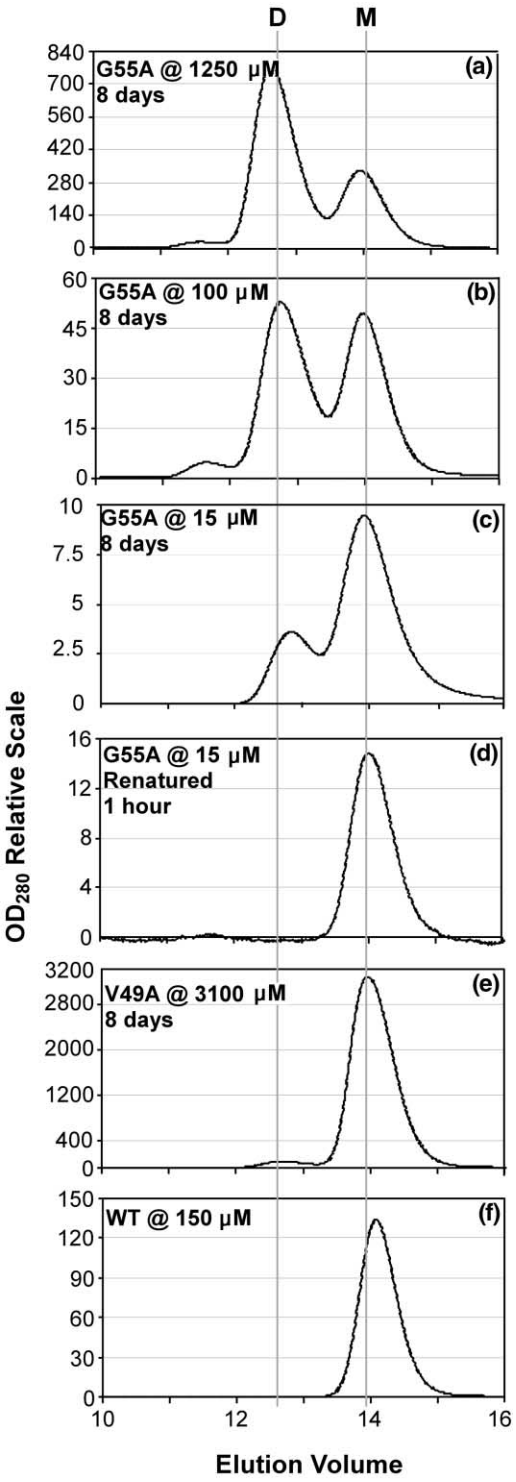


Figure 3. The Time and Protein Concentration Dependency of Domain Swapping in G55A and V49A Revealed by Size Exclusion Chromatography

(a) At the high concentration (1250 μM) G55A is primarily a dimer.

(b) Dilution of 1250 μM G55A protein to a lower concentration (100 μM) shifted the equilibrium to the monomer and resulted in an approximately equal amount of monomer and dimer.

(c) Further dilution to 15 μM resulted in an even higher percentage of the monomer over the dimer. Experiments (b) and (c) are measured after reequilibration of diluted G55A from the 1250 μM stock after 8 days. Comparing (a), (b), and (c) revealed a shift toward a higher monomer-to-dimer ratio, with a decrease in protein concentration.

(d) Freshly refolded G55A at 15 μM runs as a monomer. Comparing (d) with (c) showed that even at 15 μM there is a slow monomer-to-dimer conversion that takes days to complete.

(e) A high concentration of V49A (3100 μM) is predominantly the monomer but shows a small amount of the dimer. (f) WT runs as a monomer at the highest concentration tested. "D" and "M" represent where the dimer and monomer elute from the column. The vertical units are $OD_{280}$-relative units that reflect the overall protein concentration. The horizontal units correspond to the elution volume from the analytical Superdex-75 size exclusion column.

tact between the $C_\beta$ atom of K54 and its backbone carbonyl oxygen.

### G15A Is Strained but not Domain Swapped

Compared to G55, G15 topologically lies in a pseudo-symmetrical turn. We tested whether increasing the strain in a β turn region would be sufficient to induce domain swapping. Unlike the second β turn, the first β turn is a type I turn, with only residue G15 having a positive $\phi$ angle. As is the case for G55, the $\phi/\psi$ angle of this glycine places it in a region of $\phi/\psi$ space that is in a disallowed region of the Ramachandran plot, just outside of the allowed region for the left-handed α helices.

The Ppl G15A structure was solved at 2.1 Å resolution (Table 1) and was seen to be a monomer. This is supported by the SEC data, which suggest that G15A is monomeric in solution (data not shown). The backbone rmsd between G15A and WT* structures is only 0.41 Å, whereas the backbone rmsd is 0.75 Å between the first β turn residues (residues 13–16). The A15 residue retains the positive $\phi$ angle but now is in the allowed area of the Ramachandran plot. The $C_\beta$ of A15 clashes with the carbonyl oxygens of both A15 and N14 (Figure 7) and is likely to account for the 1.6 kcal/mol destabilization caused by the G15A mutation. The two molecules in the asymmetric unit were very similar in that they had a main-chain rmsd of 0.38 Å (residues −7–64) and 0.15 Å for their first β turns (residues 12–17).

## Discussion

The structural studies of the Ppl mutants presented here revealed that single-residue mutations to a protein with a strained β turn could lead to significant quaternary structural rearrangements in the form of 3D domain swapping.

The V49A mutation in Ppl was not expected to have a significant impact on the overall fold of the B1 domain. The V49A mutation has only a 0.92 kcal/mol destabilizing effect and was expected to cause the reorganization of the side chains in the hydrophobic core to compensate for the removal of two methyl groups. Furthermore, the effect of the V49A mutation on the folding and unfolding rates is modest. However, the structural determination led to the discovery of a 3D domain-swapping event where the fourth β strand of two Ppl monomers exchange and form an intertwined dimer. The V49A structures helped to uncover a domain-swapping mechanism

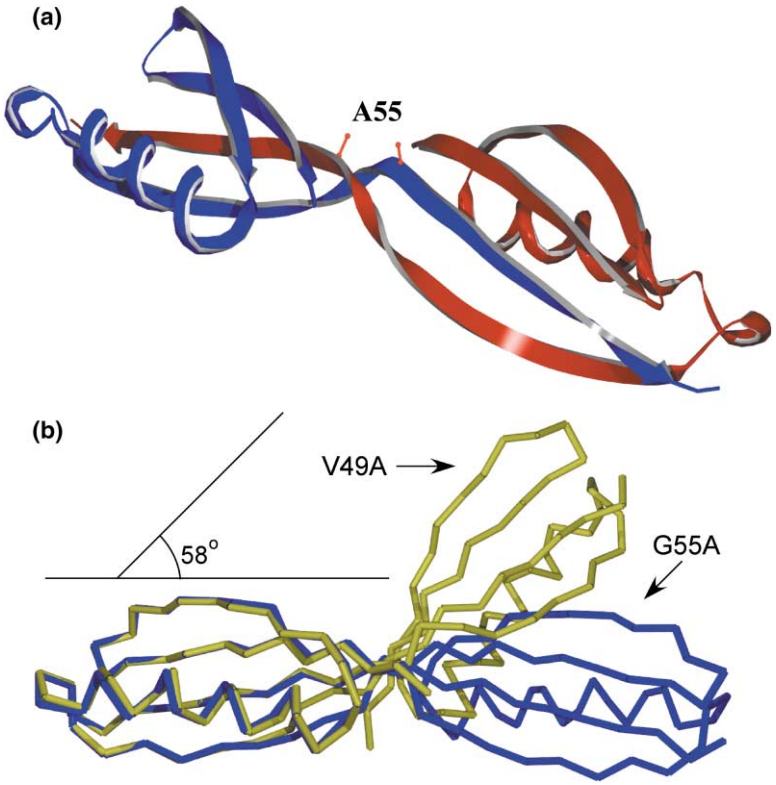


Figure 4. The G55A Domain-Swapped Dimer

(a) The G55A crystal structure reveals a domain-swapped dimer related by a crystallographic 2-fold axis. Red lines represent the $C_\alpha$ of A55. The symmetrically opposed $C_\alpha$ of A55 and its symmetry mate are 3.9 Å apart. (b) An overlay of G55A (blue) and V49A (yellow) domain-swapped dimers. The hinge angle difference is about 58° between the two monomer lobes.

in which the second β turn acts as a "spring-loaded trigger." In the second β turn of Ppl, there are three consecutive positive phi angles, two of which are non-glycines. Generally, non-glycine amino acids with positive $\phi$ angles are energetically unfavorable. The left-handed non-glycine residue has a higher conformational energy (by 1–2 kcal/mol), caused by interactions between the $C_\beta$ and main-chain atoms, than does the right-handed structure [26, 27]. Due to this conformational strain, the fourth β strand of Ppl springs open to release the strain in the second β turn when the interaction at the closed interface that holds the fourth β strand is weakened.

Both G55A and V49A fold with two-state kinetics, just as wild-type Ppl does [24]. The SEC experiments presented here revealed that freshly refolded G55A exists as monomer. Therefore, the monomeric model for G55A used in the analysis of kinetic data is valid. However, by increasing the concentration of either the V49A or especially the G55A protein creates conditions that trigger domain swapping. This is consistent with the view that local high protein concentrations can facilitate do-

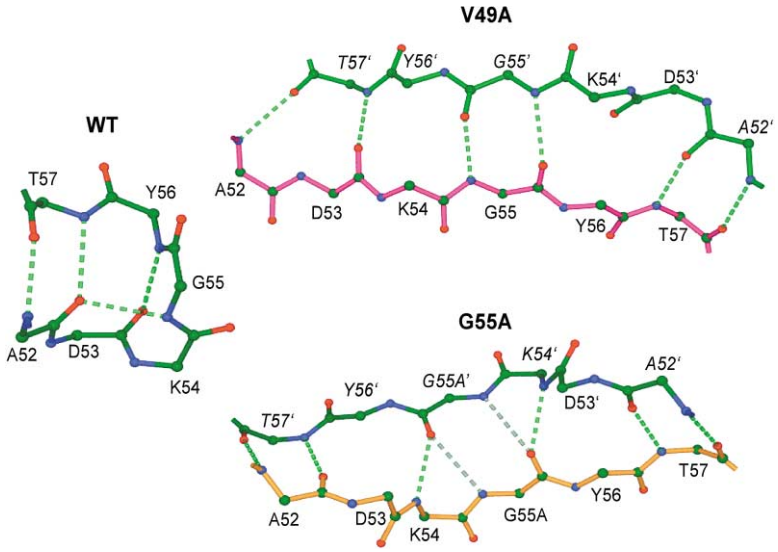


Figure 5. The Hydrogen Bonding Pattern in the Hinge-Loop Region

The hinge-loop includes residues 53–56, which in WT is the second β turn and in V49A and G55A is the hinge region. The four hydrogen bonds (H bonds) in the WT turn are shown with green dashed lines. The V49A molecule has six H bonds, whereas G55A has six H bonds with classical distances plus two long H bonds (gray dashed line) that are 3.3 Å between donor and acceptor atoms. In the V49A molecule, D53 has a positive $\phi$ angle and D53′ has a negative $\phi$ angle. This asymmetry reflects the different H bonding patterns between the V49A and G55A hinge regions.

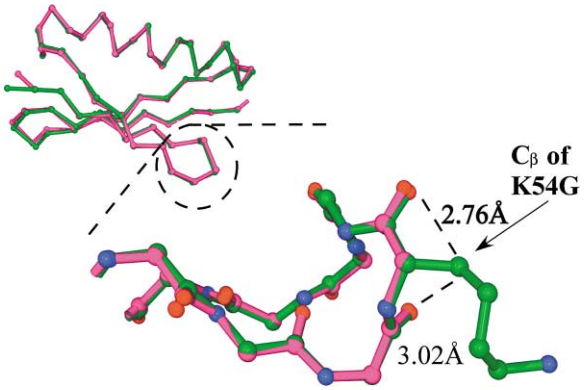


Figure 6. An Overlay of the K54G and WT* Structures

Shown in green are $C_\alpha$ representations of the WT crystal structure overlaid with the K54G structure (magenta). The K54G substitution removes the $C_\beta$-carbonyl oxygen clashing without changing the second β turn conformation. Typical distances for O-N-$C_\beta$ are 3.7–4.2 Å, and those for $C_\beta$-O are 3.0–3.4 Å, whereas in the WT* structure the $C_\beta$ and carbonyl oxygen distance is 2.76 Å.

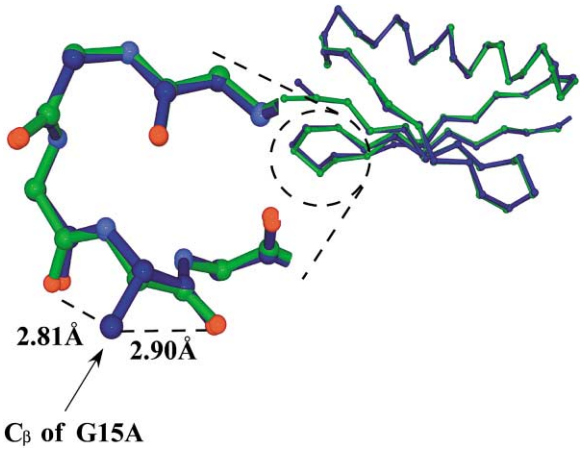


Figure 7. Overlay of G15A and WT* Structures

The G15A substitution (blue) creates unfavorable van der Waals contacts between the $C_\beta$ atom of A15 and adjacent carbonyl oxygens from A15 and N14. However, despite the additional strain G15A mutant remains monomeric. WT* is shown in green.

main swapping [8]. Thus, the G55A, as well as the V49A, mutations must destabilize the monomeric form sufficiently to cause partial or complete refolding at high protein concentrations to form a domain swapped dimer. The pH dependence has been reported for several domain-swapped proteins including Diphtheria toxin [30], and RNase A [8]. Our SEC data showed that the domain swapping process in G55A and V49A is not dependent on acidic pH but rather on concentration.

Thermodynamically, the equilibrium in domain swapping is controlled by the balance between the energy gain that is due to the strain release in the β turn and the entropic cost of dimer formation $\Delta G^{oD-M}_{Mut}$. However, the kinetic barrier should also be considered. If we assume that the monomer with the extended fourth β strand in the domain-swapped dimer mimics the conformation of the transition state, the transition state free energy can be estimated as the difference between the energy gain due to the strain release in the β turn and the energy cost of transferring the fourth β strand from the β sheet to solvent $\Delta G^{\ddagger}_{Mut}$. Since the V49A mutation caused a similar amount of local side-chain rearrangements in both the monomer and domain-swapped dimer, it can be assumed that the destabilizing effect of the V49A mutation to the monomer and to the dimer is similar (i.e., $\Delta G^{oD-M}_{V49A} \cong \Delta G^{oD-M}_{Wt}$ or $\Delta\Delta G^{oD-M}_{V49A-Wt} \cong 0$; Table 3). Therefore, it is more likely that the observed higher tendency for domain swapping in V49A as compared to the wild-type is due the lowered transition state free energy ($\Delta G^{\ddagger}_{V49A} \leq \Delta G^{\ddagger}_{Wt}$), estimated at about 1 kcal/mol (Table 3).

The destabilizing effect of the G55A mutation observed in the thermodynamic studies corresponds to the strain and steric hindrance created by the glycine-to-alanine mutation in the monomeric form of the G55A structure. Therefore, we predicted that increasing the strain in the second β turn through a G55A substitution would favor a domain-swapped state by increasing the overall stability of the dimer relative to the monomer ($\Delta G^{oD-M}_{G55A} < \Delta G^{oD-M}_{Wt}$). The theoretical free-energy difference is estimated at 2.1 kcal/mol (Table 3), favoring the dimer.

We found that strain alone in a β turn is insufficient to trigger domain swapping. This has been tested through the introduction of strain in the first β turn of Ppl. Although the G15A mutation increased the strain due to $C_\beta$ of A15 clashing with its backbone oxygen, the N-terminal first β strand does not domain swap. This is reflected in the higher estimated transition state free-energy barrier (Table 3) since the cost of removing the first β strand from the β sheet is considerably higher. Moreover, the free energy of domain swapping for the first β strand is higher compared to that for the fourth β strand since the energy gain from the release of strain in the first β turn is much smaller than that from the release of strain in the second β turn. The free-energy difference, $\Delta\Delta G^{oD-M}_{G55A-Wt}$, is estimated at −0.6 kcal/mol (Table 3), favoring the monomeric state.

Relief of the preexisting strain in the second β turn through the K54G mutation is confirmed through thermodynamic measurement and structural analysis. In the WT* structure the $C_\beta$ of K54 is only 2.8 Å away from its carbonyl oxygen, and removal of the side chain increased the stability of the protein by 0.67 kcal/mol. When the K54G structure is compared with WT*, the negligible backbone movement in the second β turn compensates little in terms of backbone motion; therefore, the increased stability is likely due to loss of the $C_\beta$-O clashing. Furthermore, a K54A mutation [24] does not increase the stability like the K54G substitution does, and thus the entropic effect of the lysine side chain can be ruled out. Since the $C_\beta$ of D53 also makes a close contact to its carbonyl oxygen because of its positive $\phi$ angle, we expect that D53 contributes to the strain in the second β turn.

Residues with positive $\phi$ angles are frequently located in turn structures [31, 32]. Takkano et al. have shown that mutations of glycines with positive $\phi$ angles in human lysozyme sometimes result in a main-chain reconfigura-

Table 3. Estimated Transition State Free Energy for Domain Swapping

| Protein | Swapped domain | $\Delta G^{\circ}_{solvation}$ (kcal/mol)[1] | $\Delta G^{\circ}_{H\text{-bonds/salt bridges}}$ (kcal/mol)[2] | $\Delta G^{\circ}_{strain}$ (kcal/mol)[3] | $\Delta G^{\ddagger}$ (kcal/mol)[4] | $\Delta\Delta G^{oD-M}_{Mut-Wt}$ (kcal/mol)[7] |
|---|---|---|---|---|---|---|
| WT model[5] | 4th β strand | 15 | 17 | 2.2 | 29.8 | – |
| V49A | 4th β strand | 14 | 17 | 2.2 | 28.8 | 0 |
| G55A | 4th β strand | 14 | 16 | 4.3 | 25.7 | 2.1 |
| G15A model[5] | 1st β strand | 11 | 26 | 1.6 | 35.4 | − 0.6 |
| DT[6] | R domain | 13 | 14 | 0 | 27 | – |

[1] Solvation energy was estimated with HYDROPHOBIC_ENERGY [44].
[2] The energy of breaking hydrogen bonds and salt bridges was estimated by the assignment of 1 kcal/mol for each hydrogen bond and salt bridge according to Schlunegger et al. [2]. The number of hydrogen bonds and salt bridges was calculated with CONTACT [45].
[3] The energy of strain was based on the change of thermodynamic stability between the mutant and wild-type for G55A, K54G, and G15A when the thermodynamic data were available. Since there was no thermodynamic data available for D53G, it was estimated as the average of the above three mutants.
[4] The transition state free energy was estimated as the sum of the solvation energy and the energy cost of breaking hydrogen bonds and salt bridges minus the energy of strain, $\Delta G^{\ddagger} = \Delta G^{\circ}_{solvation} + \Delta G^{\circ}_{H\ bonds/salt\ bridges} - \Delta G^{\circ}_{strain}$.
[5] When only a monomer structure was available, the transition state of the hypothetical dimer was modeled by rotation of the β strand out of the β sheet through the change of dihedral angles of hinge-loop residues.
[6] Data taken from Schlunegger et al. [2].
[7] The free energy of domain swapping can be estimated as the difference between the energy gain in strain release and the entropic cost of dimer formation, $\Delta G^{oD-M}_{Mut} = \Delta G^{oMut}_{strain} - \Delta G^{oMut}_{entropy}$. The free-energy difference for domain swapping between the wild-type and the mutant can be estimated as the difference between the strain energies, $\Delta\Delta G^{oD-M}_{Mut-Wt} = \Delta G^{oD-M}_{Mut} - \Delta G^{oD-M}_{Wt} \cong \Delta G^{oMut}_{strain} - \Delta G^{oWt}_{strain}$, since the entropic cost of dimer formation should be very similar between the wild-type and various mutants.

tion to compensate for the additional strain [28]. However, in both the G15A and K54G structures we saw little backbone movement with either the addition or removal of conformational strain. This suggests that in β turn structures that cannot readjust to mutations, the protein may be more prone to domain swapping.

Consecutive positive $\phi$ angles in a turn may be a useful indicator of a strain that could potentially induce domain swapping, such as in Ppl. For example, the HIV-inactivating protein, Cyanovirin-N, can domain swap under low pH or mild denaturing conditions [33]. The crystal structure of Cyanovirin-N showed that all the $\phi$ angles in the domain-swapped hinge region are negative, whereas in the NMR-derived monomeric Cyanovirin-N structure the loop region contains two positive $\phi$ angles at S52 and N53 [34]. Like those in G55A and K54G, the $C_\beta$ atoms of residues 52 and 53 in the monomeric Cyanovirin-N are making close contacts with adjacent backbone oxygens. This may lead to the domain swapping of Cyanovirin-N. However, this does not suggest that every domain-swapped oligomer has residues with positive $\phi$ angles in the monomeric form.

Other types of strained conformations in loop regions may also be good indicators of domain-swapping potential. Members of the cyclin-dependent kinase subunit family of proteins, including fission yeast p13Suc1 and human CKS1, exist in monomeric and domain-swapped forms. Bergdoll et al. [35] observed that prolines frequently exist in domain-swapped proteins. Experiments with p13Suc1 have revealed that two conserved prolines induce conformational strain in a hinge-loop and that, when these prolines are mutated to either alanines or glycines, p13Suc1 fails to domain swap [19].

Oligomerization through domain swapping has been implicated as a mechanism by which proteins may form amyloidal fibrils. A modeling paper by Sinha et al. [4] suggests that a β turn can act as a hinge-loop linking two amyloidal partners through domain swapping. For example, the amyloid-forming human Cystatin C protein (hCC), which reversibly inhibits cysteine proteases, exists as a monomer under physiological conditions. However, when hCC was crystallized, a domain-swapped dimer was observed with its second β turn as the hinge-loop, as was the case with Ppl V49A. It is thought that this is the basic unit by which the hCC amyloidal fibril forms. Also, the hCC L68Q mutation, located in the third β strand, causes a more severe incidence of amyloidal formation and can be isolated under physiological conditions as a dimer. The L68Q may lead to an increased likelihood of domain swapping by disrupting favorable hydrophobic interactions in the hydrophobic core. Interestingly, RNase A has been found to form both N-terminal [8] and C-terminal [9] domain-swapped dimers, giving it the ability to form higher-order oligomers. These findings and our own studies support domain swapping as a general mechanism for amyloid-fibril formation.

The Ppl mutant structures showed a role that hinge-loops play in the regulation of domain swapping. In many cases shortened turns or hinges restrict the access to conformations that would allow secondary-structure elements to make contacts in the same molecule. We have found that single-site mutations in the hinge-loop region also trigger domain swapping. The mild destabilization of the V49A mutation decreases the fourth β strand interactions enough that under high protein concentrations the protein domain swaps. The G55A mutation greatly increases the strain in the second β turn and creates conditions that allow the protein to first fold as a monomer, then slowly equilibrate toward a dimer. The G15A mutation did not trigger domain swapping because of the higher transition state barrier and smaller free-energy difference between the monomer and domain-swapped dimer as compared to those of G55A. The overall picture suggests that conversion of almost any protein to a domain-swapped dimer is a possibility if a sufficient amount of strain can be produced to either an N- or C-terminal α helix or β strand in a turn region. Lessons learned from our studies could be used for

designing mutants that can trigger the swapping of a specified domain in a protein.

## Biological Implications

Single-site mutations are generally thought to have only local effects on a protein structure and to primarily affect local interactions and stability. We have identified conditions in which single-site mutations in a protein can lead to significant quaternary-structural rearrangements in the form of 3D domain swapping. Domain swapping is a suitable strategy for evolving oligomers from monomers in a stepwise manner, and it also provides a plausible mechanism for the evolution of functional sites located between the monomeric units of oligomers. The formation of β-amyloid fibrils and the propagation of prion diseases are proposed to involve the process of domain swapping. However, the mechanism that controls the monomer-to-dimer conversion in domain swapping is not well understood.

The length of the hinge-loop is one of the factors that control domain swapping. Here we found another important factor that controls the monomer-dimer transition: the strain in the β turn as shown in a series of mutants of the B1 domain of Protein L. The wild-type structure showed that the second β turn contains three consecutive residues with positive $\phi$ angles that suggest this β turn is strained and perhaps "spring loaded." The preexisting strain in the second β turn is critical for inducing domain swapping either when the interactions at the closed interface that stabilize the fourth β strand are weakened (V49A) or when the strain in the β turn is further increased (G55A). Removal of a side chain (K54G) showed that the strain in the turn could be partially relieved. The thermodynamic equilibrium of domain swapping is controlled by the balance of two opposing free-energy components, the strain in the β turn versus the entropic cost of dimer formation. The kinetic barrier formed by the interactions that hold the β strand in the β sheet also affects the outcome of domain swapping. When the interactions at the closed interface are sufficiently strong, they can prevent domain swapping even when strain in the β turn is induced (G15A). The combination of single-site mutations and the preexisting strain in the second β turn demonstrates how easily any protein might form an oligomer.

## Experimental Procedures

### Protein Purification and Size Exclusion Chromatography

The cloning, expression, and purification of the tryptophan-containing B1 domain of Protein L mutant V49A was previously described [36]. The mutants G55A, K54G, and G15A were cloned and purified in a manner consistent with that presented in the study by Kim et al. [24], and references therein. The protein contains a leader His tag (numbered −7 MHHHHHHA 0), making the total length of the proteins 72 residues.

Size exclusion chromatography data were measured by the use of an analytical Superdex-75 (S75) column (Pharmacia). Sizing information for the G55A protein was obtained in the following manner: 150 μM of unfolded G55A, or WT* protein in 3 M guanidinium hydrochloride (GuHCl), was diluted 1:10 into 50 mM $NaH_2PO_4$ (pH 7.0) and then immediately injected onto a preequilibrated S75 column with 0.3 M GuHCl and 50 mM $NaH_2PO_4$. The S75 was further used for characterizing how the G55A protein equilibrates to a dimer over time. Here the protein was allowed to sit in 15 mM $NaH_2PO_4$ (pH 7.0) for 8 days at 4°C, at either 15 μM, 100 μM, or 1250 μM, and was injected onto the S75 column. Treatment of WT, V49A, and G55A under acidic conditions was as above, except that the buffer was composed of 50 mM NaOAc (pH 4.5), 150 mM NaCl, and 2 mM EDTA.

### Data Collection

All crystals were grown by the hanging-drop diffusion method. The V49A crystals were grown in 18% PEG 3350 and 0.2 M $(NH_4)_2SO_4$, 100 mM citrate (pH 4.5). The G55A crystals were grown in 225 mM ZnOAc, 2% PEG 8000, and 50 mM cacodylate (pH 6.5). The addition of 25% glycerol was utilized as a cryo-preservative for these two cases. The G15A crystals were grown in 225 mM ZnOAc and 50 mM cacodylate (pH 6.5), the K54G crystals were grown in 120 mM ZnOAc and 50 mM cacodylate (pH 6.5), and the cryo-preservative included 25% glycerol plus 5% PEG 400. All diffraction data were collected on the RAXIS-IV image plate by the use of Cu Kα radiation (λ = 1.5418 Å) generated by a RIGAKU rotating-anode generator operating at 50 kW. The data collection statistics for the crystals are summarized in Table 1.

### Structure Solution and Refinement

The programs O [37] and Xfit [38] were used for manipulations of the molecular-replacement solutions and model building. The WT* [22] structure was used as a search model for molecular replacement for all four of the mutant structures. The program EPMR [39] was utilized for molecular-replacement solutions.

During the initial model building of the V49A molecules, there were densities that lead the third β strand of B molecule into the fourth β strand of D molecules, and a conformation not consistent with WT* [22]. Following those density features in the simulated-annealing composite omit maps (Figures 2a and 2b), a model of a β strand swapped dimer was built in.

The automatic model-building features of wARP [40] were utilized for building the initial models of G55A, K54G, and G15A starting from their molecular-replacement solutions. After 100 refinement rounds and 10 building cycles, the majority of the polypeptide chains had been built for all of the molecules. The zinc ions (not included in the initial model) that were coordinated to the His tag [22] had clear electron density features on the wARP-generated $2F_o - F_c$ map (G55A, K54G, and G15A).

The program package CNS [41] was used for structural refinement, which included iterative cycles of positional, simulated-annealing, and individual B factor refinement as well as automatic water picking. The generation of a simulated-annealing composite omit $2F_o - F_c$ map after each cycle of refinement verified atomic positions and aided model rebuilding. Crystallographic refinement statistics are summarized in Table 1.

The stereochemical properties of all the mutant structures were examined by PROCHECK [42]. The quality of the main-chain and side-chain parameters were judged as mostly "better" and sometimes "inside" the normal range of comparable structures at the same resolution. The Ramachandran plot showed that the molecules in all mutant structures had at least 95% of the residues in the most-favored region (Table 1).

### Acknowledgments

We thank Dr. David Eisenberg and Dr. Yanshun Liu for discussions, suggestions, and critical reading of the manuscript. This work was supported in part by grants from the National Institutes of Health National Research Service Award T32 GM07270 and from the Fred Hutchinson Cancer Research Foundation.

Received: May 21, 2001
Revised: August 31, 2001
Accepted: September 19, 2001

### References

1. Bennett, M.J., Schlunegger, M.P., and Eisenberg, D. (1995). 3D domain swapping: a mechanism for oligomer assembly. Protein Sci. *4*, 2455–2468.

2. Schlunegger, M.P., Bennett, M.J., and Eisenberg, D. (1997). Oligomer formation by 3D domain swapping: a model for protein assembly and misassembly. Adv. Protein Chem. *50*, 61–122.
3. Fink, A.L. (1998). Protein aggregation: folding aggregates, inclusion bodies and amyloid. Fold Des *3*, R9–23.
4. Sinha, N., Tsai, C.J., and Nussinov, R. (2001). A proposed structural model for amyloid fibril elongation: domain swapping forms an interdigitating beta-structure polymer. Protein Eng. *14*, 93–103.
5. Birck, C., Vachette, P., Welch, M., Swaren, P., and Samama, J.P. (1996). Is the function of the cdc2 kinase subunit proteins tuned by their propensities to oligomerize? Conformational states in solution of the cdc2 kinase partners p13suc1 and p9cksphy. Biochemistry *35*, 5577–5585.
6. Siddhanta, U., Presta, A., Fan, B., Wolan, D., Rousseau, D.L., and Stuehr, D.J. (1998). Domain swapping in inducible nitric-oxide synthase. Electron transfer occurs between flavin and heme groups located on adjacent subunits in the dimer. J. Biol. Chem. *273*, 18950–18958.
7. Vitagliano, L., Adinolfi, S., Sica, F., Merlino, A., Zagari, A., and Mazzarella, L. (1999). A potential allosteric subsite generated by domain swapping in bovine seminal ribonuclease. J. Mol. Biol. *293*, 569–577.
8. Liu, Y., Hart, P.J., Schlunegger, M.P., and Eisenberg, D. (1998). The crystal structure of a 3D domain-swapped dimer of RNase A at a 2.1-Å resolution. Proc. Natl. Acad. Sci. USA *95*, 3437–3442.
9. Liu, Y., Gotte, G., Libonati, M., and Eisenberg, D. (2001). A domain-swapped RNase A dimer with implications for amyloid formation. Nat. Struct. Biol. *8*, 211–214.
10. Mazzarella, L., Capasso, S., Demasi, D., Di Lorenzo, G., Mattia, C.A., and Zagari, A. (1993). Bovine seminal ribuonuclease: Structure at 1.9-Å resolution. Acta Crystallogr. D *49*, 389–402.
11. Anderson, W.F., Ohlendorf, D.H., Takeda, Y., and Matthews, B.W. (1981). Structure of the cro repressor from bacteriophage lambda and its interaction with DNA. Nature *290*, 754–758.
12. Yan, Y., Winograd, E., Viel, A., Cronin, T., Harrison, S.C., and Branton, D. (1993). Crystal structure of the repetitive segments of spectrin. Science *262*, 2027–2030.
13. Tegoni, M., Ramoni, R., Bignetti, E., Spinelli, S., and Cambillau, C. (1996). Domain swapping creates a third putative combining site in bovine odorant binding protein dimer. Nat. Struct. Biol. *3*, 863–867.
14. Parge, H.E., Arvai, A.S., Murtari, D.J., Reed, S.I., and Tainer, J.A. (1993). Human CksHs2 atomic structure: a role for its hexameric assembly in cell cycle control. Science *262*, 387–395.
15. Khazanovich, N., Bateman, K., Chernaia, M., Michalak, M., and James, M. (1996). Crystal structure of the yeast cell-cycle control protein, p13suc1, in a strand-exchanged dimer. Structure *4*, 299–309.
16. Bennett, M.J., Choe, S., and Eisenberg, D. (1994). Domain swapping: entangling alliances between proteins. Proc. Natl. Acad. Sci. USA *91*, 3127–3131.
17. Green, S.M., Gittis, A.G., Meeker, A.K., and Lattman, E.E. (1995). One-step evolution of a dimer from a monomeric protein. Nat. Struct. Biol. *2*, 746–751.
18. Lapatto, R., et al., and Slingsby, C. (1991). High resolution structure of an oligomeric eye lens beta-crystallin. Loops, arches, linkers and interfaces in beta B2 dimer compared to a monomeric gamma-crystallin. J. Mol. Biol. *222*, 1067–1083.
19. Schymkowitz, J.W., Rousseau, F., and Itzhaki, L.S. (2000). Sequence conservation provides the best prediction of the role of proline residues in p13suc1. J. Mol. Biol. *301*, 199–204.
20. Rousseau, F., Schymkowitz, J.W., Wilkinson, H.R., and Itzhaki, L.S. (2001). Three-dimensional domain swapping in p13suc1 occurs in the unfolded state and is controlled by conserved proline residues. Proc. Natl. Acad. Sci. USA *98*, 5596–5601.
21. Wikström, M., Drakenberg, T., Forsén, S., Sjöbring, U., and Björck, L. (1994). Three-dimensional solution structure of an immunoglobulin light chain-binding domain of protein L. Comparison with the IgG-binding domains of protein G. Biochemistry *33*, 14011–14017.
22. O'Neill, J.W., Kim, D.E., Baker, D., and Zhang, K.Y.J. (2001). Structures of the B1 domain of protein L from Peptostreptococcus magnus with a tyrosine to tryptophan substitution. Acta Crystallogr. D *57*, 480–487.
23. Gu, H., Kim, D., and Baker, D. (1997). Contrasting roles for symmetrically disposed beta-turns in the folding of a small protein. J. Mol. Biol. *274*, 588–596.
24. Kim, D.E., Fisher, C., and Baker, D. (2000). A breakdown of symmetry in the folding transition state of protein L. J. Mol. Biol. *298*, 971–984.
25. Ramachandran, G.N., and Sasisekharan, V. (1968). Conformation of polypeptides and proteins. Adv. Protein Chem. *23*, 283–438.
26. Stites, W.E., Meeker, A.K., and Shortle, D. (1994). Evidence for strained interactions between side-chains and the polypeptide backbone. J. Mol. Biol. *235*, 27–32.
27. Kimura, S., Kanaya, S., and Nakamura, H. (1992). Thermostabilization of Escherichia coli ribonuclease HI by replacing left-handed helical Lys95 with Gly or Asn. J. Biol. Chem. *267*, 22014–22017.
28. Takano, K., Yamagata, Y., and Yutani, K. (2000). Role of amino acid residues at turns in the conformational stability and folding of human lysozyme. Biochemistry *39*, 8655–8665.
29. Singh, J., and Thornton, J.M. (1990). SIRIUS. An automated method for the analysis of the preferred packing arrangements between protein groups. J. Mol. Biol. *211*, 595–615.
30. Bennett, M.J., Choe, S., and Eisenberg, D. (1994). Refined structure of dimeric diphtheria toxin at 2.0 Å resolution. Protein Sci. *3*, 1444–1463.
31. Richardson, J.S. (1981). The anatomy and taxonomy of protein structure. Adv. Prot. Chem. *34*, 167–339.
32. Thornton, J.M., Sibanda, B.L., Edwards, M.S., and Barlow, D.J. (1988). Analysis, design and modification of loop regions in proteins. Bioessays *8*, 63–69.
33. Yang, F., et al., and Wlodawer, A. (1999). Crystal structure of cyanovirin-N, a potent HIV-inactivating protein, shows unexpected domain swapping. J. Mol. Biol. *288*, 403–412.
34. Bewley, C.A., et al., and Gronenborn, A.M. (1998). Solution structure of cyanovirin-N, a potent HIV-inactivating protein. Nat. Struct. Biol. *5*, 571–578.
35. Bergdoll, M., Remy, M.H., Cagnon, C., Masson, J.M., and Dumas, P. (1997). Proline-dependent oligomerization with arm exchange. Structure *5*, 391–401.
36. Johnsen, K., O'Neill, J.W., Kim, D.E., Baker, D., and Zhang, K.Y.J. (2000). Crystallization and preliminary X-ray diffraction studies of mutants of B1 IgG-binding domain of protein L from Peptostreptococcus magnus. Acta Crystallogr. D *56*, 506–508.
37. Jones, T.A., Zou, J.Y., Cowan, S.W., and Kjeldgaard, M. (1991). Improved methods for building protein models in electron density maps and the location of errors in these models. Acta Crystallogr. A *47*, 110–119.
38. McRee, D.E. (1992). A visual protein crystallographic software system for X11/XView. J. Mol. Graph. *10*, 44–46.
39. Kissinger, C.R., Gehlhaar, D.K., and Fogel, D.B. (1999). Rapid automated molecular replacement by evolutionary search. Biol. Crystallogr. D *55*, 484–491.
40. Perrakis, A., Sixma, T.K., Wilson, K.S., and Lamzin, V.S. (1997). wARP—improvement and extension of crystallographic phases by weighted averaging of multiple-refined dummy atomic models. Acta Crystallogr. D *53*, 448–455.
41. Brünger, A.T., et al., and Warren, G.L. (1998). Crystallography & NMR system: a new software suite for macromolecular structure determination. Acta Crystallogr. D *54*, 905–921.
42. Laskowski, R.A., MacArthur, M.W., Moss, D.S., and Thornton, J.M. (1993). PROCHECK: a program to check the stereochemical quality of protein structures. J. Appl. Cryst. *26*, 283–291.
43. Brünger, A.T. (1992). Free *R* value: a novel statistical quantity for assessing the accuracy of crystal structures. Nature *355*, 472–475.
44. Eisenberg, D., and McLachlan, A.D. (1986). Solvation energy in protein folding and binding. Nature *319*, 199–203.
45. CCP4 (Collaborative Computational Project 4) (1994). The CCP4 suite: programs for protein crystallography. Acta Crystallogr. D *50*, 760-763.

**Accession Numbers**

The atomic coordinates for the four Ppl mutants, V49A, G55A, K54G, and G15A, have been deposited in the Protein Data Bank with accession codes 1K50, 1K51, 1K52, and 1K53, respectively.